Published in final edited form as:
Science. 2011 December 23; 334(6063): 1713–1716. doi:10.1126/science.1210770.

Mismatch repair, but not heteroduplex rejection, is temporally coupled to DNA replication

Hans Hombauer, **Anjana Srivatsan**, **Christopher D. Putnam**, and **Richard D. Kolodner**
Ludwig Institute for Cancer Research, Departments of Medicine and Cellular and Molecular Medicine and Cancer Center, Moores-UCSD Cancer Center, and the Institute of Genomic Medicine, University of California School of Medicine, San Diego 9500 Gilman Drive, La Jolla, CA 92093-0669

Abstract

In eukaryotes, it is unknown if mismatch repair (MMR) is temporally coupled to DNA replication and how strand-specific MMR is directed. Here we fused *Saccharomyces cerevisiae MSH6* with cyclins to restrict the availability of the Msh2-Msh6 mismatch recognition complex to either S-phase or G2/M. The Msh6-S cyclin fusion was proficient for suppressing mutations at three loci that replicate at mid-S-phase, whereas the Msh6-G2/M cyclin fusion was defective. However, the Msh6-G2/M cyclin fusion was functional for MMR at a very late-replicating region of the genome. In contrast, the heteroduplex rejection function of MMR during recombination was partially functional during both S-phase and G2/M. These results indicate a temporal coupling of MMR, but not heteroduplex rejection, to DNA replication.

DNA mismatch repair (MMR) recognizes mispairs in DNA caused by DNA replication errors, and targets the newly synthesized DNA strand for repair by an excision and resynthesis mechanism (1-3). MMR repair is initiated by the recognition of the mispair by the MutS homodimer in bacteria and the MutS-related Msh2-Msh6 and Msh2-Msh3 heterodimers in eukaryotes, which possess differing mispair-binding specificities (4, 5). Identification of the newly synthesized DNA strand in *Escherichia coli* MMR is mediated by nicking of the newly synthesized, unmethylated strand by MutH at hemi-methylated GATC sites in response to a mispaired base (2). The critical hemi-methylated sites are generated by replication of methylated chromosomal DNA and provide a temporal post-replication window for repair that closes when the Dam methylase modifies the newly synthesized DNA strand. Whether MMR in eukaryotes is coordinated with DNA replication is less clear. The replication clamp PCNA functions in MMR (6) and both Msh6 and Msh3 contain N-terminal binding sites for PCNA providing the potential for coupling of mismatch recognition to the replication machinery (7, 8). Despite this, *msh6* and *msh3* mutations that specifically eliminate PCNA binding cause very weak MMR defects (7-9), which in the case of Msh6 reflects the functional redundancy of the Msh6 PCNA binding site with other regions of the Msh6 N-terminus whose roles are not yet understood (9). To directly test temporal coupling of MMR with DNA replication, we restricted the availability of the Msh2-Msh6 mispair recognition complex to specific stages of the cell cycle of *S. cerevisiae msh3*Δ mutants.

Functional Msh6 fusions with controlled cell cycle expression were generated by fusing different cyclins to the Msh6 N-terminus at the *MSH6* chromosomal locus and replacing the *MSH6* promoter with the cell cycle-regulated cyclin promoter (Figure 1A). A fusion of *MSH6* with a fragment of *CLB6* encoding the first 195 residues under control of the *CLB6*

Address correspondence to: Richard D. Kolodner, rkolodner@ucsd.edu, (858) 534-7804 (phone), (858) 822-4479 (fax).

promoter, *S-MSH6*, restricted Msh6 expression primarily to between 20 and 50 minutes after release from alpha-factor arrest (Figure 1B). This expression period corresponded to S-phase as demonstrated by FACS (Figure 1B). We also constructed a fusion of *MSH6* to a fragment of *CLB2* encoding the first 181 residues under control of the *CLB2* promoter and encoding the L26A mutation that prevents nuclear export (10) similar to the *CLB2* fusions used to study post-replication repair (11). This fusion, *G2/M-MSH6*, restricted Msh6 expression to primarily after 40 minutes after release from alpha-factor arrest, which was during G2/M-phase based on FACS analysis (Figure 1B). We were unable to construct a G1 phase restricted *MSH6* gene that expressed sufficient Msh6 to allow testing on MMR in G1.

We introduced the *S-MSH6* and *G2/M-MSH6* fusion constructs into a strain containing an *msh3*Δ mutation to eliminate any repair mediated by the partially redundant Msh2-Msh3 heterodimer (4, 5). We then measured the rates of reversion of the *hom3-10* and *lys2-10A* frameshift mutations and inactivation of the *CAN1* gene (Figure S1A), which are elevated in MMR-defective mutants. The mutation rates of the *S-MSH6 msh3*Δ strain were substantially lower than the fully MMR-defective *msh6Δ msh3*Δ strain in all three MMR assays, indicating that this fusion construct was functional *in vivo* (Table 1). The mutation rates of the *S-MSH6 msh3*Δ strain were, however, slightly higher than that of the *msh3*Δ strain, possibly due to the reduced expression of S-Msh6 relative to Msh6 (Figure 1B). In contrast, the mutation rates of the *G2/M-MSH6 msh3*Δ strain were equivalent to that of the MMR-defective *msh6Δ msh3*Δ strain in all three MMR assays (Table 1), indicating that restricting Msh6 expression to G2/M-phase prevented MMR at the loci tested.

The *G2/M-MSH6* construct could be inactive due to the nature of the fusion protein or due to the restricted expression of Msh6 in G2/M. To distinguish between these possibilities, a version of the Clb2-Msh6 fusion, *G2/M-deg$_{mut}$-MSH6*, was generated that was expressed throughout the cell cycle (Figure 1B). Three modifications of the *G2/M-MSH6* construct were required to obtain expression throughout the cell cycle: replacement of the *CLB2* promoter with the *MSH6* promoter, deletion of the destruction box (D-box) located at amino acids 25-33 and mutation of the KEN$_{100}$-box degron that control ubiquitin-mediated degradation at the end of mitosis and in G1 (12, 13) (Figure 1A). The *G2/M-deg$_{mut}$-MSH6 msh3*Δ strain had mutation rates that were similar to the *msh3*Δ strain and were substantially lower than the *msh6Δ msh3*Δ strain (Table 1). The slightly higher mutation rates of the *G2/M-deg$_{mut}$-MSH6 msh3*Δ strain relative to the *S-MSH6 msh3*Δ strain is consistent with observed expression levels of the G2/M-deg$_{mut}$-Msh6 protein and the S-Msh6 protein (Figure 1B). These results indicate that the N-terminal Clb2 fusion *per se* does not compromise the function of Msh6 and that the failure of G2/M-Msh6 to support MMR is due to its G2/M restricted expression. Thus, expression of Msh6 during S-phase is required for functional MMR at the *hom3-10, lys2-10A* and *CAN1* loci, and the capability of these loci to be repaired by MMR is lost some time between 40 and 60 minutes after release from alpha-factor arrest.

The average times of replication for the *hom3-10, lys2-10A,* and *CAN1* loci are 32, 39, and 33 minutes, respectively, after release from alpha-factor arrest (14). These times are within the time window of the bulk of genome replication (Figure S2) and during the peak expression of *S-MSH6* but not *G2/M-MSH6*. We reasoned that if the difference between *S-MSH6* and *G2/M-MSH6* in the MMR assays were due to temporal coupling between MMR and DNA replication, then *G2/M-MSH6* might be functional during MMR in late replicated regions of the genome. We chose one of the latest replicating non-telomeric regions of the genome (14), which is on chromosome IV adjacent to the *POL3* and *DUN1* genes with an average replication time of 49 minutes (Figure S2) and moved the *lys2-10A* assay to this location in an *msh3*Δ strain, generating *lys2-10A$_{LATE}$*. We did not move the other MMR assays as *hom3-10* is linked to an origin of replication and the *CAN1* inactivation assay

could identify other types of gene-inactivating events, like chromosomal rearrangements, depending on chromosomal context (15). Expression of the wild-type *MSH6* allele resulted in the same low mutation rate in both the *lys2-10A*$_{LATE}$ and the *lys2-10A* frameshift reversion assays (Table 1) (p=0.14); in contrast, the *G2/M-MSH6* allele was completely defective for suppressing the frameshift reversion rate of *lys2-10A* (372-fold increase in mutation rate) (p=0.5) but almost completely suppressed the frameshift reversion rate of *lys2-10A*$_{LATE}$ (11-fold increase in mutation rate). Additionally, the *S-MSH6* allele, which had weak Msh6 expression at 50 minutes (Figure 1B), was significantly more defective for MMR at the *lys2-10A*$_{LATE}$ locus than the *G2/M-MSH6* allele (p=0.0001), but was not completely defective compared to the *msh3Δ msh6*Δ double mutant (p=0.002). As expected, the mutation rates of the native-positioned and earlier replicating *hom3-10* and *CAN1* loci were reduced to a low level by the *S-MSH6* allele but not *G2/M-MSH6* allele in the *lys2-10A*$_{LATE}$ strain. Thus, these data indicate that the *G2/M-MSH6* allele was functional and could mediate MMR at late replicating loci but not at early replicating loci, further supporting a temporal coupling of MMR with DNA replication.

In addition to roles in MMR, Msh2-Msh6 and Msh2-Msh3 suppress recombination between closely related, but non-identical (homeologous) substrates, a process termed heteroduplex rejection (16-18). We introduced the *G2/M-MSH6* and *S-MSH6* alleles into *msh3*Δ strains containing an assay, which monitors the formation of His$^+$ prototrophs mediated by recombination between 100% identical (homologous) or between 91% identical (homeologous) substrates (16) (Figure S1B). With wild-type *MSH6*, recombination was strongly biased towards homologous recombination indicating that heteroduplex rejection was functional (Table 2). In contrast, this bias was strongly reduced when *MSH6* was deleted, indicating that the *msh6*Δ mutation caused a defect in heteroduplex rejection. Both the *G2/M-MSH6* and *S-MSH6* alleles were partially functional and equivalent in the suppression of homeologous recombination, despite the fact that the assay was integrated at the *URA3* locus, which has an average replication time of 28 minutes (14). Similarly, both the *G2/M-MSH6* and *S-MSH6* alleles were able to suppress the formation of translocations mediated by homeologous recombination between a segmental duplication region on chromosome V and targets on chromosomes IV, X, and XIV (18) (Figure S1C). In this assay, the *G2/M-MSH6* allele resulted in a greater decrease in the rate of translocations mediated by homeologous recombination relative to that caused by the *S-MSH6* allele, although the 95% confidence intervals of the two rates overlapped (Table 3). These results indicate that heteroduplex rejection is mediated to an equivalent extent by Msh6 expressed in both S and G2/M and does not appear to be dependent upon replication timing, in contrast to MMR. This is similar to prior observations of MMR acting on mispaired bases in meiotic and mitotic recombination intermediates after DNA replication has been completed and in mitotic recombination intermediates formed prior to DNA replication (1, 19).

Restriction of Msh6 expression during the cell cycle through fusion to cyclins has revealed a strong temporal coupling between DNA replication and mismatch repair, but a lack of temporal coupling for heteroduplex rejection. This temporal coupling is likely due to the regulation or appearance of a signal for repair and is not due to the regulation of the MMR proteins. We have recently shown that Msh2-Msh6 dependent MMR involves two mispair recognition pathways, one in which Msh2-Msh6 is stably recruited to replication factories through the Msh6-PCNA interaction and a second Msh6-PCNA interaction independent pathway (20). Furthermore, Msh2-Msh6 dependent MMR is completely dependent on the PCNA coupling of Msh2-Msh6 to replication factories in *exo1* mutants (20). Thus PCNA may provide a physical signal for coupling of one of the MMR pathway to the replication fork, whereas the signal for the second MMR pathway is unknown. Other possibilities for the repair signals are single-stranded gaps and nicks transiently generated by DNA replication (21), which is consistent with the requirement for a nick in MMR *in vitro* (22,

23). The signals triggering MMR on mitotic and meiotic recombination intermediates and for initiating heteroduplex rejection, which differs from MMR due to modified protein requirements (16, 24, 25), are presently unclear but could be nicks, gaps, branched structures or the mispairs in the DNA intermediates.

Supplementary Material

Refer to Web version on PubMed Central for supplementary material.

Acknowledgments

This study was supported by NIH grant GM50006 (to R.D.K.).

References

1. Harfe BD, Jinks-Robertson S. Annu Rev Genet. 2000; 34:359.
2. Iyer RR, Pluciennik A, Burdett V, Modrich PL. Chem Rev. 2006; 106:302. [PubMed: 16464007]
3. Kolodner RD, Marsischky GT. Curr Opin Genet Dev. 1999; 9:89.
4. Marsischky GT, Filosi N, Kane MF, Kolodner R. Genes Dev. 1996; 10:407.
5. Sia EA, Kokoska RJ, Dominska M, Greenwell P, Petes TD. Mol Cell Biol. 1997; 17:2851. [PubMed: 9111357]
6. Chen C, Merrill BJ, Lau PJ, Holm C, Kolodner RD. Mol Cell Biol. 1999; 19:7801. [PubMed: 10523669]
7. Flores-Rozas H, Clark D, Kolodner RD. Nat Genet. 2000; 26:375. [PubMed: 11062484]
8. Clark AB, Valle F, Drotschmann K, Gary RK, Kunkel TA. J Biol Chem. 2000; 275:36498.
9. Shell SS, Putnam CD, Kolodner RD. Mol Cell. 2007; 26:565. [PubMed: 17531814]
10. Hood JK, Hwang WW, Silver PA. J Cell Sci. 2001; 114:589. [PubMed: 11171327]
11. Karras GI, Jentsch S. Cell. 2010; 141:255.
12. Hendrickson C, Meyn MA 3rd, Morabito L, Holloway SL. Curr Biol. 2001; 11:1781. [PubMed: 11719221]
13. Wasch R, Cross FR. Nature. 2002; 418:556. [PubMed: 12152084]
14. Raghuraman MK, et al. Science. 2001; 294:115.
15. Chen C, Umezu K, Kolodner RD. Mol Cell. 1998; 2:9. [PubMed: 9702187]
16. Datta A, Adjiri A, New L, Crouse GF, Jinks Robertson S. Mol Cell Biol. 1996; 16:1085. [PubMed: 8622653]
17. Matic I, Rayssiguier C, Radman M. Cell. 1995; 80:507. [PubMed: 7859291]
18. Putnam CD, Hayes TK, Kolodner RD. Nature. 2009; 460:984. [PubMed: 19641493]
19. Orr-Weaver TL, Szostak JW. Microbiol Rev. 1985; 49:33. [PubMed: 3884994]
20. Hombauer H, Campbell CS, Smith CE, Desai A, Kolodner RD. Cell. 2011 in press.
21. Langston LD, O#x2019;Donnell M. Mol Cell. 2006; 23:155.
22. Zhang Y, et al. Cell. 2005; 122:693.
23. Constantin N, Dzantiev L, Kadyrov FA, Modrich P. J Biol Chem. 2005; 280:39752. [PubMed: 16188885]
24. Sugawara N, Goldfarb T, Studamire B, Alani E, Haber JE. Proc Natl Acad Sci U S A. 2004; 101:9315. [PubMed: 15199178]
25. Myung K, Datta A, Chen C, Kolodner RD. Nat Genet. 2001; 27:113.
26. Janke C, et al. Yeast. 2004; 21:947. [PubMed: 15334558]
27. Amin NS, Nguyen MN, Oh S, Kolodner RD. Mol Cell Biol. 2001; 21:5142. [PubMed: 11438669]

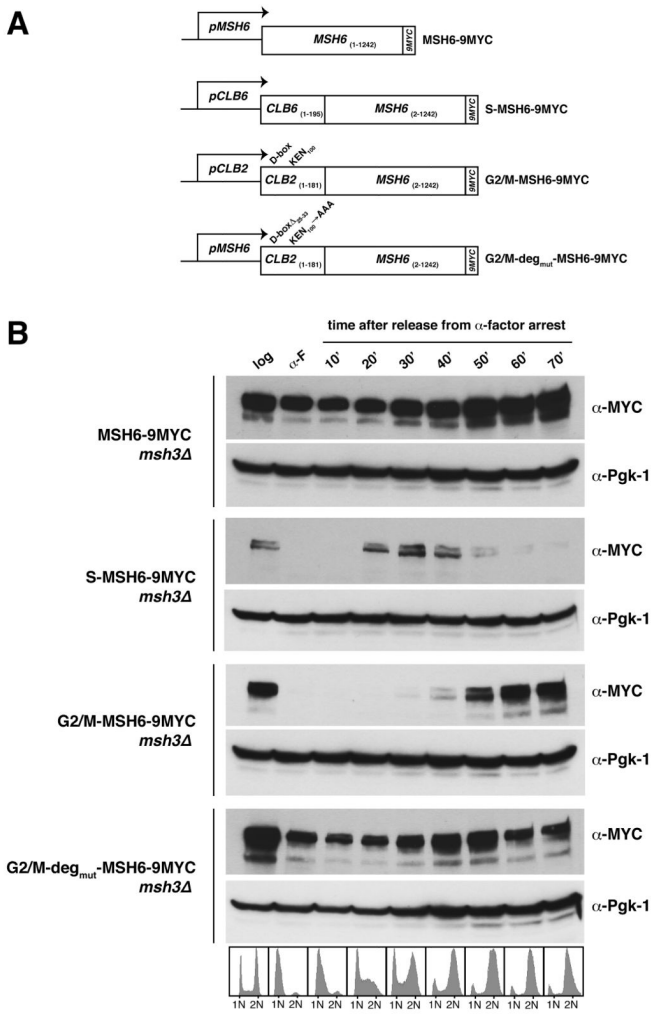

Figure 1.

A. Diagrams of tagged *MSH6* constructs. B. (Top) Expression level of Msh6 revealed by Western blots of whole cell lysates with anti-Myc antibodies for log-phase cells (log), alpha-factor arrested cells (α-F), and cells released from alpha-factor arrest for the indicated times. An anti-Pgk1 blot is shown as a loading control. (Bottom) FACS profiles of cells showing the cell cycle distribution at the indicated time points. The FACS profile displayed is for the *MSH6-9MYC msh3*Δ strain; however, all of the strains used had essentially identical profiles.

Table 1
MMR repair activity during S and G2/M stages of the cell cycle

		Mutation rate (fold increase)*		
Relevant genotype	**Strain RDKY**	***Thr*** $^{+}$	***Lys*** $^{+}$	**Can^{R}**
*msh3*Δ	7672	5.1 [3.4-6.4] × 10^{-8} (1)	7.8 [6.0-11.3] × 10^{-8} (1)	8.0 [6.2-16.8] × 10^{-8} (1)
*msh3*Δ *msh6*Δ	7674	5.5 [3.6-8.6] × 10^{-6} (108)	3.3 [2.2-4.6] × 10^{-5} (423)	2.4 [1.6-3.8] × 10^{-6} (30)
*G2/M-MSH6 msh3*Δ	7676	4.3 [3.3-5.5] × 10^{-6} (84)	2.9 [1.7-4.7] × 10^{-5} (372)	2.9 [2.1-4.3] × 10^{-6} (36)
*S-MSH6 msh3*Δ	7678	6.9 [4.8-8.9] × 10^{-7} (13)	2.6 [1.8-4.0] × 10^{-6} (33)	4.1 [3.1-5.1] × 10^{-7} (5)
*G2/M-deg$_{mut}$-MSH6 msh3*Δ	7680	2.5 [1.1-3.1] × 10^{-7} (5)	3.9 [1.5-5.0] × 10^{-7} (5)	2.1 [1.6-3.4] × 10^{-7} (3)
*msh3*Δ *lys2-10A$_{LATE}$*	7681	4.8 [2.3-5.9] × 10^{-8} (1)	1.1 [0.6-2.5] × 10^{-7} (1)	9.7 [5.2-12.5] × 10^{-8} (1)
*msh3*Δ *msh6*Δ *lys2-10A$_{LATE}$*	7688	4.8 [2.5-10.8] × 10^{-6} (93)	7.3 [2.1-11.1] × 10^{-5} (932)	2.1 [1.0-2.8] × 10^{-6} (26)
*G2/M-MSH6 msh3*Δ *lys2-10A$_{LATE}$*	7682	3.4 [2.5-4.2] × 10^{-6} (68)	8.8 [5.3-17.9] × 10^{-7} (11)	1.8 [1.0-2.4] × 10^{-6} (22)
*S-MSH6 msh3*Δ *lys2-10A$_{LATE}$*	7684	8.1 [5.6-10] × 10^{-7} (16)	1.2 [0.8-1.8] × 10^{-5} (155)	3.2 [1.9-4.4] × 10^{-7} (4)

*Median rates of *hom3-10 (Thr^{+})* and *lys2-10A (Lys^{+})* reversion and inactivation of *CAN1* (Can^{R}) with 95% C.I. in square brackets and fold increase relative to the *msh3*Δ strain in parentheses.

Table 2

MMR suppression of homeologous recombination during S and G2/M

	Inverted repeat recombination rate (His+) (fold increase)*				
	100% homologous substrate		91% homeologous substrate		
Relevant genotype	**Strain RDKY**	**Rate**	**Strain RDKY**	**Rate**	**Ratio 91/100†**
*msh3*Δ	7672	3.9 [3.0-5.2] × 10^{-6} (1)	7673	2.6 [1.9-3.0] × 10^{-7} (1)	0.07
*msh3*Δ *msh6*Δ	7674	3.6 [3.3-4.8] × 10^{-6} (0.9)	7675	1.4 [1.3-1.6] × 10^{-6} (5.4)	0.39
*G2/M-MSH6 msh3*Δ	7676	5.8 [4.4-9.1] × 10^{-6} (1.5)	7677	7.8 [5.0-10.2] × 10^{-7} (3)	0.13
*S-MSH6 msh3*Δ	7678	4.7 [3.8-6.2] × 10^{-6} (1.2)	7679	7.9 [6.3-11.8] × 10^{-7} (3)	0.17

*Inverted repeat recombination rate (*His*$^{+}$) with 95% C.I. in square brackets. The number in parentheses represents the fold increase relative to the *msh3*Δ strain rate for each respective recombination substrate.

†The inverted repeat recombination rate for the 91% homeologous substrate divided by the inverted repeat recombination rate for the 100% homologous substrate.

Science. Author manuscript; available in PMC 2013 October 23.

Table 3

MMR suppression of duplication mediated GCRs during S- and G2/M

Relevant genotype	Strain RDKY	GCR rate* (fold increase)
wild-type	6678	4.13 [3.1-6.6] × 10^{-8} (1)
*msh6*Δ	6714	2.18 [1.6-2.7] × 10^{-7} (5.3)
G2/M-MSH6	7685	4.00 [2.8-7.4] × 10^{-8} (1.0)
S-MSH6	7686	9.11 [5.7-16.4] × 10^{-8} (2.2)

*Rate of $5FOA^R$ Can^R progeny. The number in parentheses represents the fold increase relative to the wild-type GCR rate.